



Article

Optimizing Voltage Stability in Distribution Networks via Metaheuristic Algorithm-Driven Reactive Power Compensation from MDHD EVs

Chen Zhang ^{1,*}, Kouros Sedghisigarchi ², Rachel Sheinberg ¹, Shashank Narayana Gowda ¹ and Rajit Gadh ¹

¹ Smart Grid Energy Research Center, Mechanical and Aerospace Engineering Department, University of California, Los Angeles, CA 90095, USA; rsheinberg@g.ucla.edu (R.S.); shashank07@ucla.edu (S.N.G.); rgadh@seas.ucla.edu (R.G.)

² Electrical and Computer Engineering Department, California State University, Northridge, CA 91330, USA; ksedghi@csun.edu

* Correspondence: chenzhang96@g.ucla.edu

Abstract: The deployment of medium-duty and heavy-duty (MDHD) electric vehicles (EVs), characterized by their substantial battery capacity and high charging power demand, poses a potential threat to voltage stability within distribution networks. One possible solution to voltage instability is reactive power compensation from charging MDHD EVs. However, this process must be carefully facilitated in order to be effective. This paper introduces an innovative distribution network voltage stability solution by first identifying the network's weakest buses and then utilizing a metaheuristic algorithm to schedule reactive power compensation from MDHD EVs. In the paper, multiple metaheuristic algorithms, including genetic algorithms, particle swarm optimization, moth flame optimization, salp swarm algorithms, whale optimization, and grey wolf optimization, are subjected to rigorous evaluation concerning their efficacy in terms of voltage stability improvement, power loss reduction, and computational efficiency. The proposed methodology optimizes power flow with the salp swarm algorithm, which was determined to be the most effective tool, to mitigate voltage fluctuations and enhance overall stability. The simulation results, conducted on a modified IEEE 33 bus distribution system, convincingly demonstrate the algorithm's efficacy in augmenting voltage stability and curtailing power losses, supporting the reliable and efficient integration of MDHD EVs into distribution networks.

Keywords: MDHD EVs; voltage stability; reactive power compensation; metaheuristic algorithms



Citation: Zhang, C.; Sedghisigarchi, K.; Sheinberg, R.; Narayana Gowda, S.; Gadh, R. Optimizing Voltage Stability in Distribution Networks via Metaheuristic Algorithm-Driven Reactive Power Compensation from MDHD EVs. *World Electr. Veh. J.* **2023**, *14*, 310. <https://doi.org/10.3390/wevj14110310>

Academic Editor: Zhaoyun Zhang

Received: 12 October 2023

Revised: 10 November 2023

Accepted: 13 November 2023

Published: 15 November 2023



Copyright: © 2023 by the authors. Licensee MDPI, Basel, Switzerland. This article is an open access article distributed under the terms and conditions of the Creative Commons Attribution (CC BY) license (<https://creativecommons.org/licenses/by/4.0/>).

1. Introduction

Amidst a growing urgency to cut down on greenhouse gas emissions and shift towards more environmentally friendly modes of transportation [1,2], the electrification of medium-duty and heavy-duty (MDHD) trucks has emerged as a crucial part of the transition. According to the International Energy Agency (IEA), the global fleet of electric MDHD trucks is projected to approach 4 million units by the year 2030 [3]. In the United States, California has taken a pioneering stance by mandating that 75% of all Class 4–8 straight truck sales within the state must be zero-emission by 2035 [4], with more stringent requirements continuing to be proposed. However, the integration of these MDHD electric vehicles into existing distribution networks introduces a set of intricate challenges, including hosting capacity constraints and voltage stability issues [5]. This complexity is exacerbated by the substantial battery capacities and increased charging power demands characteristic of MDHD EVs, both of which can threaten the stability of distribution grids [6]. MDHD vehicles, often charged collectively at depot facilities due to the operational nature of commercial fleets, pose a set of challenges distinct from their light-duty counterparts, which are more commonly charged separately across residential neighborhoods [3]. Consequently,

distribution system operators must prepare to address the unique charging requirements associated with MDHD EVs.

As a result, tackling the incorporation of MDHD EVs or entire electric vehicle fleets into the power grid has become a prominent research focus. In a study by Hong et al. [7], automated electrified freight transportation systems were simulated to evaluate the repercussions of interactions between electrified mobility and the grid. Their findings indicate that automation significantly reduces costs and peak loads, both of which posed challenges for human-driven MDHD EVs. In a separate study by Vandael et al. [8], the authors introduce a cost-effective day-ahead consumption plan for an EV fleet, relying on reinforcement learning techniques. Other research endeavors delve into the necessary charging infrastructure requirements for MDHD EVs, underscoring the importance of strategically siting high-power charging stations to ensure the economic feasibility of MDHD EV integration [9].

The aforementioned studies, however, do not address the potential voltage stability issues that accompany large-scale MDHD EV charging. One solution to voltage instability, especially that caused by the integration of distributed energy resources (DERs), is reactive power compensation [10]. Reactive power is essential for maintaining voltage levels within acceptable bounds [11] and can help counteract voltage drops and fluctuations that may occur due to changes in load or other system disturbances [12]. Thus, generating and managing reactive power effectively is a fundamental aspect of maintaining the reliability of an electrical power system. Traditional methods of reactive power management have included capacitor-based solutions such as shunt compensation [13].

More recently, however, a field of research has emerged to study the use of DERs themselves for reactive power compensation. For example, some studies focus on the use of battery energy storage systems—such as the authors in [14], who utilize a voltage stability evaluation model to coordinate real and reactive compensation from battery energy storage. In [15], the authors propose voltage control through a decentralized architecture that can coordinate active and reactive power injections by DERs. Others focus on the use of renewable energy resources for reactive power compensation. For example, in [11], the authors utilize both shunt capacitors and distributed wind generation, facilitated by static and dynamic analyses, to support voltage stability on the distribution network. In [16], the authors utilize a two-part control scheme to manage reactive power injection from a grid-integrated solar photovoltaic (PV) inverter. Finally, the authors in [17] exploit the flexibility of PVs to inject and absorb reactive power in order to stabilize voltage in areas of dense EV charging.

It is also possible for EVs to provide reactive power compensation. Research on advanced EV chargers that operate in full four quadrants has enabled a broader view of EV charging with both active and reactive power [18,19]. The newest studies demonstrate that EVs can provide an efficient way to support power grids with reactive power. In [20], the authors propose an efficient control strategy and novel EV charger to enable EVs to inject reactive power into the grid. In [21], the authors utilize a model predictive control method to enable EVs to act as reactive power compensation devices and mitigate voltage instability. In [22], the authors assess the voltage violation risks in distribution networks considering the reactive power response of smart inverters including both EV and PV chargers. However, the locations of the smart chargers are randomly assigned and there is no voltage profile provided after the reactive power compensation.

Our study builds on previous work on EV reactive power compensation to specifically consider the challenges of integrating MDHD EVs. We aim to optimize the power flow within the distribution network, with the goal of minimizing voltage fluctuations at individual bus locations that host MDHD EV charging infrastructure. This optimization is executed by exploiting the reactive power compensation potential of MDHD EVs, facilitated through the utilization of four-quadrant chargers [23] during high-power depot charging sessions.

In order to accomplish this task, it is crucial to coordinate the reactive power injections via an optimization algorithm that can produce voltage stabilization solutions in

a computationally efficient manner. Previous research has explored the use of various optimization strategies for voltage stabilization and for EV charging scheduling more broadly. For example, many researchers have turned to metaheuristic algorithms for optimization. Metaheuristic algorithms are a class of optimization techniques used to solve complex problems for which traditional mathematical or algorithmic methods may not be efficient or applicable [24]. These algorithms are designed to explore and exploit solution spaces effectively, often inspired by natural phenomena or human behavior [25]. Unlike specific problem-solving algorithms, metaheuristics provide a flexible framework that can be adapted to a wide range of optimization challenges including the optimal power flow problem [26]. Therefore, they can be extremely useful in regulating reactive power compensation from MDHD EVs.

Although MDHD EVs are a relatively new topic for research, utilizing metaheuristics for EV charging does have precedence in the literature. For example, the authors in [27] utilize a metaheuristic called the water cycle algorithm to minimize the price and peak load of light-duty EV charging, taking advantage of reactive power compensation from the vehicles. In [28], a metaheuristic called particle swarm optimization is utilized to facilitate both PV and light-duty EV reactive power injections into the grid, highlighting the need for optimization in reactive power compensation problems. Lastly, the authors in [29] utilize an improved mixed real and binary vector-based swarm optimization to coordinate high-penetration EV charging and maintain energy and voltage stability in a distribution grid. However, although this study includes impressive case studies, it does not consider four-quadrant EV charging, does not investigate MDHD EVs, and does not explore more than one optimization algorithm. Table 1 compares the solutions explored in the reactive power compensation literature.

Table 1. Comparison of reactive power compensation research in the literature.

Ref	Reactive Power Provider	Optimization Algorithm
[14]	Battery storage	Single metaheuristic algorithm (PSO)
[15]	DERs	Lagrange multipliers
[11]	Shunt capacitors, wind	Deterministic method
[16]	PVs	Closed-loop control
[20–22]	Regular EVs	Closed-loop control, MPC control, N/A
Our paper	MDHD EVs	Multiple metaheuristic algorithms

Our proposed methodology explores and compares the capabilities of multiple metaheuristic algorithms. We have carefully evaluated an assortment of metaheuristics to determine which may be the most effective in stabilizing distribution network voltage. The tested algorithms include the genetic algorithm [30], particle swarm optimization [31], moth flame optimization [32], the salp swarm algorithm [33], whale optimization [34], and grey wolf optimization [35]. The specific evaluation criterion considers the capacity of these metaheuristic algorithms to augment voltage stability, curtail power losses, and exhibit computational efficiency.

The goals of this paper are to first identify the most sensitive buses in a power distribution network which may have the highest impact on voltage profile deviation and power loss reduction and then to conduct reactive power compensation from MDHD EVs at the identified buses while the EVs are charging. This problem is formulated to minimize voltage magnitude deviation at individual bus locations and is solved by a metaheuristic algorithm. We apply and investigate several metaheuristic algorithms to determine which provides the optimal solution with a thorough evaluation over three dimensions—voltage deviation, power losses, and computational time.

The main contributions of this study are (1) an analysis of the influence of MDHD EVs' depot charging on power distribution network voltage stability; (2) the employment of a novel approach that first identifies the weakest buses of the distribution network and then harnesses reactive power compensation from MDHD EVs via a metaheuristic algorithm;

(3) the mitigation of voltage deviation and power loss on the distribution network while utilizing only 20% of the inverter capacity of MDHD EVs; and (4) the comprehensive evaluation of a range of metaheuristic algorithms across various dimensions, all geared towards improving voltage stability.

The subsequent sections of this paper are structured as follows: in Section 2, we delve into the problem formulation, which encompasses the system model and optimization objectives. This section also introduces our novel approach rooted in metaheuristic algorithms and includes an overview of each of the algorithms that have been tested. Section 3 is dedicated to the presentation of the simulation results, and it includes a comprehensive discussion of the evaluated algorithms and their ability to regulate reactive power compensation. Section 4 concludes the paper and explores future research directions.

2. Problem Formulation

2.1. Problem Statement

Voltage deviation is a key metric that functions as a barometer for both the stability and caliber of electrical power provisioning within a distribution network. Deviations can be caused by fluctuations in load demand, oscillations in renewable energy generation, and imbalances in reactive power.

MDHD EVs exhibit a pronounced appetite for high charging power, spanning from 150 kW to 400 kW during depot charging and increasing up to 1.2 MW for on-the-move charging scenarios [36]. Due to their high charging power demand, MDHD charging loads will have a significant negative impact on voltage stability and correspondingly power loss in the distribution network. However, the extensive battery capacities characterizing MDHD EVs, ranging from 80 kWh to 550 kWh [37], coupled with the deployment of four-quadrant chargers, empower these vehicles to make significant injections of reactive power back into the grid. We propose an approach to utilize up to 20% of the inverter capacity for reactive power compensation. This approach first identifies the weakest buses of the distribution network and then aims to mitigate any voltage instability through the reactive power-enabled MDHD vehicle charging. The flowchart of the proposed approach is shown in Figure 1.

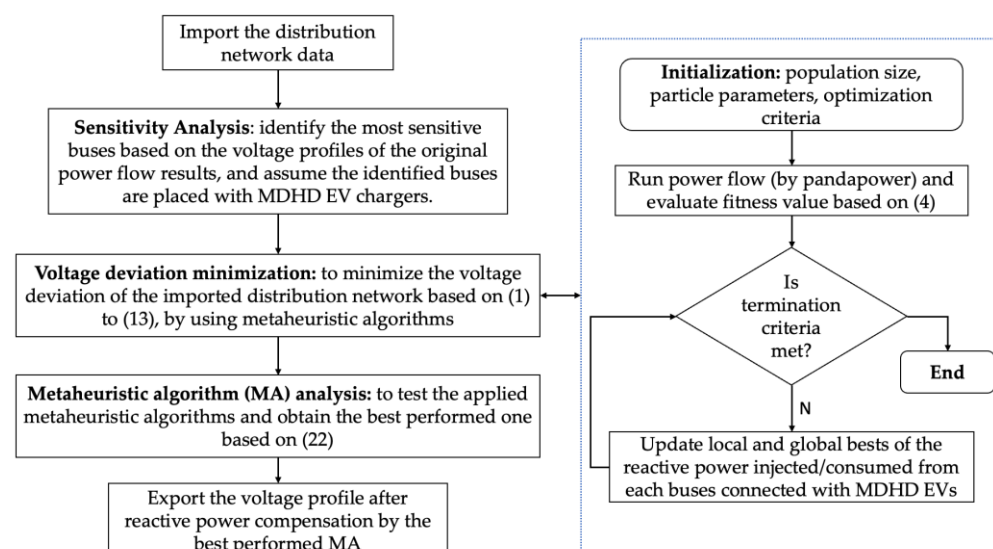


Figure 1. Flowchart of the proposed approach.

2.2. Optimization Objective and Constraints

In the proposed research, we determine the optimal amount of reactive power consumed/generated by individual buses connected with MDHD EVs to minimize the voltage magnitude deviation while still adhering to the intricate operational, equality, and in-

equality constraints intrinsic to the power grid's dynamics [30]. This can be formulated as the following:

$$\text{Min } F(x, u), \quad (1)$$

Subject to

$$h_i(x, u) = 0 \quad i = 1, 2, 3, \dots, m, \quad (2)$$

$$g_j(x, u) \leq 0 \quad j = 1, 2, 3, \dots, n, \quad (3)$$

where F is the objective function, x and u are the state variables vector and the control variables vector, h_i and g_j are the equality and inequality constraints, and m and n are the number of constraints.

The objective of this research is to reduce voltage deviation at each bus in the distribution network; thus, (1) can be rewritten as:

$$\text{Min} \sum_{l=1}^L \left(|V_l| - |V_{ref}| \right)^2, \quad (4)$$

where V_l is the voltage magnitude at bus l , V_{ref} is the reference voltage value per unit, set as 1, and L is the total number of buses.

The balanced power flow equations are represented as equality constraints in the following manner:

$$P_{Gi} - P_{Li} = |V_i| \left[\sum_{j=1}^L |V_j| [G_{ij} \cos(\delta_i - \delta_j) + B_{ij} \sin(\delta_i - \delta_j)] \right], \quad (5)$$

$$Q_{Gi} - Q_{Li} = |V_i| \left[\sum_{j=1}^L |V_j| [G_{ij} \sin(\delta_i - \delta_j) - B_{ij} \cos(\delta_i - \delta_j)] \right], \quad (6)$$

where P_{Gi} and Q_{Gi} are the generated active and reactive power, P_{Li} and Q_{Li} are the active and reactive load demands at bus i . V_i and V_j are the voltage magnitudes at bus i and j . δ_i and δ_j are the voltage angles at bus i and j . G_{ij} and B_{ij} are the conductance and susceptance of the bus line ij .

The inequality constraints primarily pertain to the operational limitations of the generators, transformers, and power ratings of MDHD EVs and are categorized as follows:

Generator constraints:

$$P_{Gi}^{min} \leq P_{Gi} \leq P_{Gi}^{max} \quad i = 1, 2, \dots, N_G, \quad (7)$$

$$V_{Gi}^{min} \leq V_{Gi} \leq V_{Gi}^{max} \quad i = 1, 2, \dots, N_{PV}, \quad (8)$$

$$Q_{Gi}^{min} \leq Q_{Gi} \leq Q_{Gi}^{max} \quad i = 1, 2, \dots, N_{PV}, \quad (9)$$

Transformer constraints:

$$T_i^{min} \leq T_i \leq T_i^{max} \quad i = 1, 2, \dots, N_T, \quad (10)$$

Security constraints:

$$V_i^{min} \leq V_i \leq V_i^{max} \quad i = 1, 2, \dots, N_{PQ}, \quad (11)$$

EV constraints:

$$P_i^{EV2} + Q_i^{EV2} \leq S_i^{EV2} \quad i = 1, 2, 3, \dots, N_{EV}, \quad (12)$$

$$Q_i^{EV} \leq 0.2 * S_i^{EV} \quad i = 1, 2, 3, \dots, N_{EV}, \quad (13)$$

where N_G is the number of generators, N_{PV} is the number of PV buses, N_C is the number of shunt compensators, Q_{Ci} is the injected reactive power from shunt compensators at bus i , T_i^{min} and T_i^{max} are the minimum and the maximum limits to the tap setting of transformers, N_T is the number of the transformers, V_i^{min} and V_i^{max} are the minimum and maximum voltage limits of load bus i , N_{PQ} is the number of load buses, S_i is the cumulative apparent power of EV chargers at bus i , and N_{EV} is the number of buses connecting to MDHD EVs.

It is worth mentioning that within the scope of this study, we have classified the loads into two distinct categories: EV loads, comprising MDHD EVs, and non-EV loads. For the EV loads, we have introduced a power constraint for each EV charger to guarantee its correct operation within the four-quadrant range, represented in Equation (12). Furthermore, we have enforced a restriction on the amount of reactive power, ensuring that it does not surpass 20% of the socket rating, as shown in Equation (13), thus fulfilling the energy demands of the MDHD EVs before they embark on their trips [38].

2.3. Metaheuristic Algorithms

The optimization problem is tackled using a range of metaheuristic algorithms, with the control variables designated as the reactive power injected into the grid from MDHD EVs at their respective bus locations. In this section, we provide an overview of the metaheuristic algorithms that have been employed and assessed in this study.

2.3.1. Genetic Algorithm

The genetic algorithm (GA), originally introduced in the 1970s, is a robust metaheuristic approach inspired by the principles of natural selection and genetics. It has found extensive applications in the field of optimal power flow [30]. GA initiates its operation with an initial population of potential solutions, each assessed using a fitness function. Through the mechanisms of selection, crossover, and mutation, successive generations of solutions are generated, progressively enhancing their fitness. The algorithm iteratively explores the search space for optimal solutions by evolving the population across multiple generations. In our investigation, the fitness function aligns with the objective function represented by Equation (4).

2.3.2. Particle Swarm Optimization

Particle swarm optimization (PSO), a metaheuristic optimization algorithm introduced in 1995, has been readily applied in the realm of optimal power flow [31]. It emulates the dynamics of a swarm of particles navigating a search space. In this context, each particle symbolizes a potential solution, and the algorithm continuously refines the particles' positions and velocities by considering their individual best-known positions and the global best-known position within the swarm. This coordinated movement facilitates the exploration of the search space and the gradual convergence towards optimal solutions.

For each particle i , the position update equation is as follows:

$$p_i(t+1) = p_i(t) + v_i(t+1), \quad (14)$$

The velocity update equation of PSO is shown in (16).

$$v_i(t+1) = w \cdot v_i(t) + c_1 \cdot r_1 [p_i^*(t) - p_i(t)] + c_2 \cdot r_2 [p_i^{g*}(t) - p_i(t)], \quad (15)$$

where w is the inertia weight, r_1 and r_2 are random values in the range of $[0, 1]$, c_1 and c_2 are acceleration constants, $p_i^*(t)$ is the best position of particle i at time t , and $p_i^{g*}(t)$ is the global best position of the entire swarm at time t .

2.3.3. Moth Flame Optimization

Moth flame optimization (MFO), introduced in 2013, has likewise found application in addressing optimal power flow challenges [32]. Drawing inspiration from the navigational

behavior of moths attracted to light sources, MFO models each moth as a potential solution. It encapsulates the spiral movement of a moth as it approaches a flame. Within the framework of MFO, candidate solutions correspond to these moths, with their positions in the search space serving as the control variables. The mathematical representation of MFO is shown in Equation (16).

$$MFO = (I, P, T), \quad (16)$$

where I refers to the first random locations of the moths, P refers to the motion of the moths in the search space, and T refers to the outcome of the search process (true or false). Details of I , P , and T can be found in Taher et al.'s research [32].

2.3.4. Salp Swarm Algorithm

The salp swarm algorithm (SSA), introduced as a metaheuristic optimization algorithm in 2017 [33], takes inspiration from the collective behavior of salp organisms in nature. The SSA emulates these creatures' movement and interactions to address optimization challenges. In the mathematical representation of salp chains, the population is initially categorized into two groups: the leader and the followers. The leader represents the salp at the front of the chain, while the rest of the salps are considered followers. An equation, as presented below, governs the continued updating of the leader's position in relation to the food source.

$$p_j^1 = \begin{cases} F_j + c_1((U_j - L_j)c_2 + U_j)c_3 \geq 0 \\ F_j - c_1((U_j - L_j)c_2 + U_j)c_3 < 0' \end{cases} \quad (17)$$

where, U_j and L_j are the upper and lower limits of the control variables in the j th dimension. F_j is the position of the food source, c_1 is a time variable coefficient, and c_2 and c_3 are random variables within $[0, 1]$. The equations of Newton's laws of motion are utilized to update the positions of the followers.

2.3.5. Whale Optimization Algorithm

The whale optimization algorithm (WOA), initially presented in 2016 [34], draws inspiration from the hunting strategies of humpback whales. WOA mimics the movement and communication patterns among these whales to address optimization challenges. In WOA, some whales venture into the search space randomly, promoting exploration, while others gravitate towards a prey (the best solution found thus far) to encourage exploitation. The algorithm employs specific equations to update the positions of the whales, facilitating both effective exploration and convergence toward optimal solutions. An equation that captures the helix-shaped movement observed in humpback whales' behavior is employed to guide their motion, as depicted below.

$$p_i(t+1) = D \cdot e^{bl} \cdot \cos(2\pi l) + p_i^*(t), \quad (18)$$

where D is the distance of the i th whale to the prey (best solution found so far), b is the constant for defining the shape of the logarithmic spiral, l is the random number within $[-1, 1]$, and $p_i^*(t)$ is the position vector of the best solution obtained so far.

2.3.6. Grey Wolf Optimization

Grey wolf optimization (GWO) is a metaheuristic algorithm introduced in 2014 [35]. This metaheuristic algorithm emulates the collaborative and communicative behavior of wolves to tackle optimization challenges. Within GWO, the population is segregated into alpha, beta, delta, and omega wolves, symbolizing the best-known solutions. The algorithm preserves the top three solutions obtained thus far and compels the remaining search agents to adjust their positions in accordance with the best-performing agents. This process is exemplified by the equations provided below.

$$D_\alpha = |C_1 \cdot P_\alpha - P|, D_\beta = |C_2 \cdot P_\beta - P|, D_\delta = |C_3 \cdot P_\delta - P|, \quad (19)$$

$$P_1 = P_\alpha - A_1 \cdot D_\alpha, P_2 = P_\beta - A_1 \cdot D_\beta, P_3 = P_\delta - A_1 \cdot D_\delta, \quad (20)$$

$$P(t+1) = (P_1 + P_1 + P_1)/3, \quad (21)$$

where P is the position vector of a grey wolf, A and C are coefficient vectors, and $D = |C \cdot P^*(t) - P(t)|$ with $P^*(t)$ is the position vector of the prey [12].

2.4. Performance Evaluation

Furthermore, we introduce a performance index denoted as I to assess the performance of the metaheuristic algorithms. Its definition is presented below. The performance of these algorithms is evaluated on three dimensions: voltage variation (\tilde{V}), power loss (PL), and computational time (CT). A lower I value signifies superior performance in the evaluation criteria.

$$I = w_1 \cdot \tilde{V} + w_2 \cdot PL + w_3 \cdot CT, \quad (22)$$

where w represents the weight allocated to the three factors, denoting their respective significance in selecting the most suitable algorithm for implementation.

3. Simulation Results and Discussions

We utilized the modified IEEE 33 bus system [39] as our experimental framework to analyze and evaluate the impact of MDHD EV charging, as facilitated by the aforementioned metaheuristic algorithms, on the voltage stability of distribution networks. For power flow modeling, we make use of pandapower [40]. Our assessment involves quantifying the voltage stability improvements achieved through the proposed approach and conducting a comparative analysis of the aforementioned metaheuristic algorithms.

We found that the most sensitive buses for each branch of the IEEE 33 bus distribution network are buses 18, 25, and 33, which have the weakest voltage. The reactive power compensation is conducted by assuming MDHD EVs are connected to these identified buses. The original load flow results of the IEEE 33 bus distribution system are shown in Appendix A Table A1 for reference.

3.1. Simulation Settings

According to the study in [37], we configured the active charging power of each MDHD EV charger to fall within the range of 300 kW to 350 kW, ensuring that it aligns with the energy requirements of the users. Moreover, we set the maximum socket rating of these chargers to 1.2 MVA. Our scenario involves the presence of four depots for MDHD EVs, situated at buses numbered 18, 22, 25, and 33, as illustrated in Figure 1. Each of these depots is equipped with two chargers. It is important to note that the capability for reactive power compensation is exclusive to four-quadrant chargers. In our simulation, we assume that four-quadrant chargers are available in depots connected to buses 18, 25, and 33, while the depot at bus 22 does not possess this capability. We focus our analysis on the most demanding scenario, where MDHD EVs at different buses are charging concurrently. The configuration of the IEEE bus distribution system and the locations of the MDHD EV chargers are shown in Figure 2.

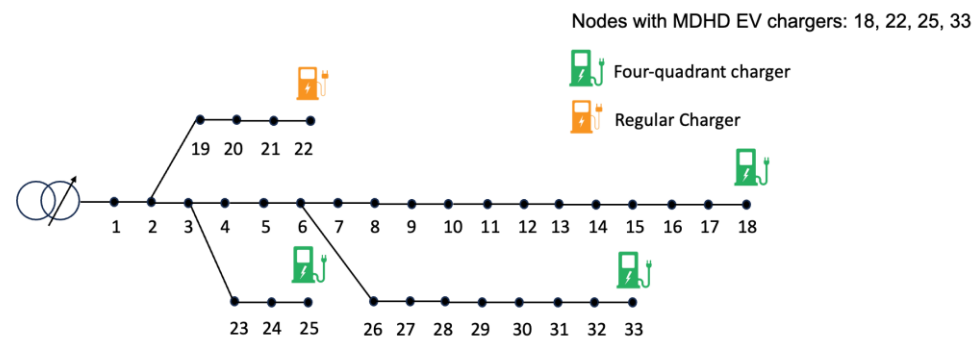


Figure 2. Modified IEEE 33 bus distribution system with the location of MDHD EV chargers.

3.2. Metaheuristic Algorithm Analysis

In this case study, we employed the metaheuristic algorithms detailed in Section 2 to address voltage stability enhancement in the IEEE 33 bus system. The primary objective is to regulate the injection of reactive power from MDHD EVs into the grid using four-quadrant chargers. For consistency and equitable evaluation, we set weights w_1 , w_2 , and w_3 as 0.5, 0.3, and 0.2, respectively, to calculate the performance index I . Our values for the weights, combined with the larger range of computational time when measured in seconds, were chosen due to the significance of efficiency in scheduling MDHD EV charging in the future [41]. To ensure robust and unbiased assessments, each algorithm is subject to 30 implementations, with subsequent averaging of the three key factors: \tilde{V} , PL , and CT . This averaging procedure mitigates the impact of inherent randomness. Furthermore, all algorithms share common stopping criterion during optimization, defined as the requirement that the difference between consecutive iterations remains below 10^{-6} . The general parameters for the metaheuristic algorithms such as population size are set identically and are listed in Table 2.

Table 2. Parameter values for metaheuristic algorithms.

Parameters	Values
Population size	50
Maximum iterations	100
Termination criteria	10^{-6}

Figure 3 provides an overview of the voltage deviation values, also referred to as fitness values, derived from the algorithms across 30 implementations. Additionally, it offers insights into the convergence pattern of these values within a single implementation. In Figure 3, it is evident that the fitness values of WOA exhibit considerable variation across implementations, with it being distinct from the others. Meanwhile, Figure 4 highlights that PSO and GWO exhibit the highest and lowest initial fitness values in one implementation, respectively. It is crucial to note that PSO, under the specified settings, does not consistently converge within the maximum iteration times. Thus, large penalty values can occur under the non-converged implementations of PSO, which are represented in the large value of the averaged voltage variation in Table 3. Consequently, the voltage deviation value for PSO is omitted from Figure 4, with it differing from the presentation of the other algorithms, due to the substantial penalty value applied to its total fitness value.

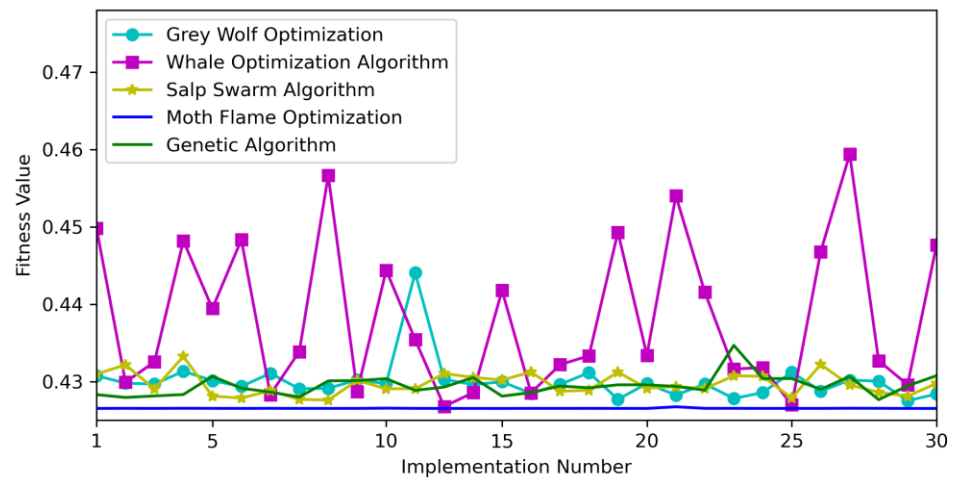


Figure 3. The voltage deviation values of various algorithms across 30 implementations.

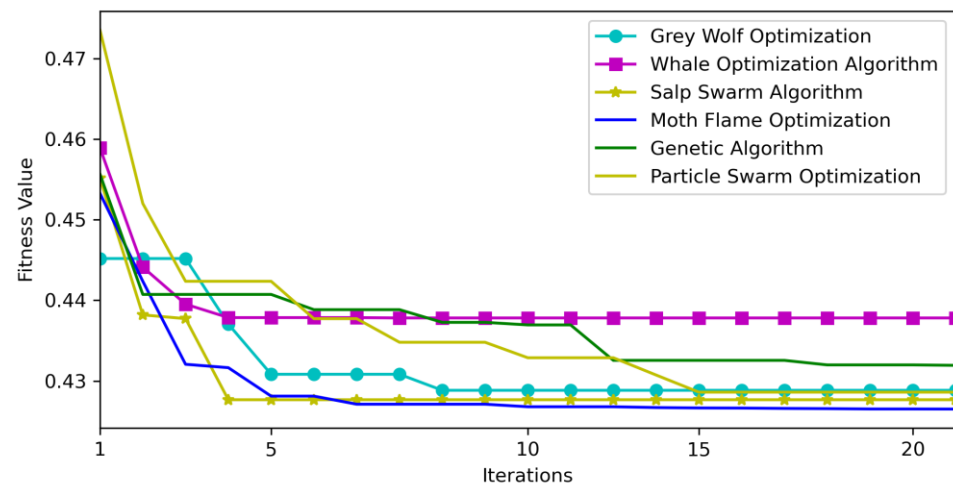


Figure 4. The voltage deviation values of different algorithms for the first 20 iterations within a single implementation.

Table 3. Average values for the voltage variation, power loss, and computational time of the different metaheuristic algorithms.

	$Av_{\tilde{V}}$ (p.u.)	Av_{PL} (p.u.)	Av_{CT} (s)	I
GA	0.4294	0.4037	418.6772	84.0716
PSO	117.09 (penalized value)	0.4063	221.1575	102.8984
MFO	0.4265	0.4031	621.9836	124.3309
SSA	0.4296	0.4046	40.1610	8.3683
WOA	0.4383	0.4101	217.5731	43.8586
GWO	0.4300	0.4042	83.2494	16.9861

Table 3 presents a comparative analysis of the algorithms’ performance. Notably, MFO demonstrates exceptional results by achieving the lowest voltage deviation and power loss. However, it comes at the cost of extended computational time, surpassing 621 s. On the other hand, SSA showcases remarkable efficiency, completing computations in roughly 40 s, while still maintaining competitive values for voltage deviation and power loss. These attributes make SSA particularly well-suited for practical implementation, as supported by its favorable overall performance score of 8.3683, according to the proposed performance index I .

3.3. Voltage Stability Results

Based on our analysis, the salp swarm algorithm (SSA) emerges as the most effective metaheuristic algorithm. Therefore, we proceed to apply the SSA in the subsequent section, which discusses the results related to voltage stability. In Figure 5, the voltage magnitude at each bus is depicted across different scenarios. The yellow line represents the voltage magnitude in the original power flow when MDHD EVs do not consume active power. The blue line illustrates the voltage profile during MDHD EVs' charging sessions, while the dark green line showcases the voltage profile when reactive power compensation is employed. Notably, certain buses experience a significant voltage drop when MDHD EV loads from various buses connect to the grid simultaneously without reactive power compensation. However, with the implementation of reactive power compensation, the voltage magnitude is substantially improved and better aligned with the original voltage levels. It is worth mentioning that this voltage stability enhancement is achieved through the assumption that only three buses have limited reactive power compensation (20%). To achieve more substantial voltage profile improvement (such as ± 0.05 p.u. deviation), we could either add more buses with chargers for reactive power compensation or increase the amount of reactive power from each MDHD EV inverter.

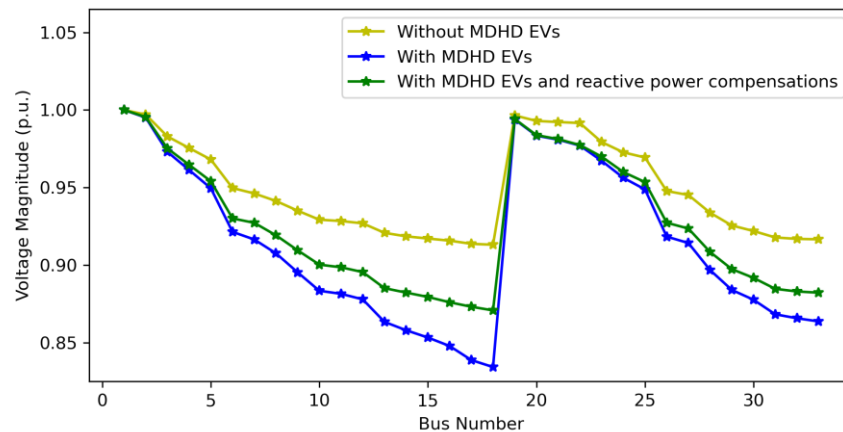


Figure 5. Voltage magnitude profile of the 33-bus system with/without MDHD EVs and with MDHD EVs plus reactive power compensation.

Table 4 provides a comprehensive breakdown of voltage deviation and power loss within the three scenarios. The outcomes illustrate the considerable improvements achieved in voltage stability and power loss reduction compared to the scenario where MDHD EVs are integrated into the grid without the benefit of reactive power compensation. It shows 15.13% enhancement for voltage deviation and 11.73% improvement for power loss after reactive power compensation.

Table 4. Voltage variation and power loss.

	No MDHD EVs	MDHD EVs	MDHD EVs with Reactive Power Compensation	Improved Percentage
Voltage variation	0.3421 p.u.	0.5055 p.u.	0.4291 p.u.	15.13%
Power loss	0.2026 p.u.	0.4692 p.u.	0.4142 p.u.	11.73%

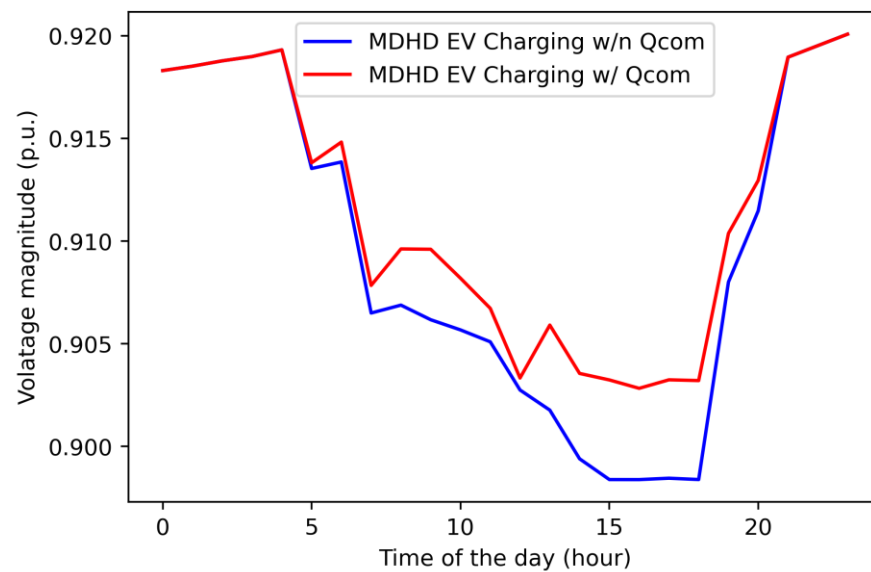
With the application of our algorithm, the specific quantities of reactive power injected into the grid by the MDHD EV chargers located at the three EV buses are shown in Table 5.

Table 5. Reactive power injection at different buses.

Bus Number	Reactive Power (kVar)
11	448.11
20	380.75
33	479.61

We also studied the time-series voltage profile of the modified IEEE 33 bus with reactive power support provided by MDHD EVs while satisfying the charging demand with a randomly given arrival and departure time of the vehicles during a day. The data for non-EV loads were sourced from the End-Use Load Profiles for U.S. Building Stock developed by the National Renewable Energy Laboratory. The data represent 2% of the overall electricity consumption and cover a span of 24 h in July 2018. This dataset encompasses electricity usage in 60 residential buildings, along with two small office buildings and two retail strip malls situated in West Los Angeles [42].

Figure 6 illustrates the voltage magnitude profile at bus 11 over the course of a day. The red line represents the voltage profile during MDHD EV charging sessions with reactive power compensation, whereas the blue line represents the profile without such compensation. The data are indicative of a significant difference; with reactive power compensation, the voltage magnitude remains consistently above 0.9 at bus 11. Conversely, in the absence of reactive power compensation, the voltage magnitude falls below 0.9, negatively impacting the stability of the distribution network.

**Figure 6.** Voltage magnitude profile of bus 11 with/without reactive power compensation from MDHD EVs.

In discussing these voltage stability results, we also want to return to the weights of the performance index: the selection of the best performing metaheuristic algorithm is based on the performance index I in Equation (22). In this study, we emphasize the significance of computational time ($w_3 = 0.2$) over the other two factors—voltage deviation ($w_1 = 0.5$) and power loss ($w_2 = 0.3$), given the potential need for the timely execution of charging scenarios for MDHD EVs in the future. In this paper, the weight of computational time is 0.2, but when considering the unit difference between time (seconds) and voltage deviation (p.u.) and power loss (p.u.), respectively, the effect of computational time is highlighted and then voltage deviation and finally power loss. Nevertheless, the weight distribution can be flexibly adjusted to align with specific operator requirements or preferences.

It is also worth mentioning that this voltage stability enhancement is achieved by only assuming three buses with limited reactive power compensation (20%). To achieve

more robust voltage profile improvement, more buses with chargers for reactive power compensation or an increased amount of reactive power from each MDHD EV inverter are required. Further research can be conducted to investigate the performance of the proposed approach with different reactive power capacity limits while still satisfying the charging demand of the MDHD EV owners through smart charging strategies.

The findings from this research not only provide valuable insights, but also useful directives for the assimilation of MDHD EVs into distribution networks. Our approach optimizes their charging strategy in order to support grid stability. Future research endeavors may gravitate toward the development of an intelligent charging algorithm, calibrated to meet the precise energy needs of MDHD EVs. This future approach would encompass the dual objectives of transportation energy demand fulfillment and voltage stability enhancement within distribution networks.

4. Conclusions

This study aids in establishing a more robust energy system by harnessing MDHD EVs' reactive power compensation potential. The proposed approach first identifies the weakest buses of the power distribution network and then selects the best performing metaheuristic algorithm to minimize the voltage magnitude deviation of the distribution network. The selection of the SSA as the most efficient metaheuristic algorithm is driven by the anticipation of a future demand for rapid MDHD EV charging scenarios. The findings of this investigation offer insights into a possible solution for the smooth assimilation of MDHD EVs into distribution networks, ensuring their effective use while upholding grid stability.

Author Contributions: Conceptualization, C.Z. and K.S.; methodology, C.Z., K.S. and R.S.; software, C.Z.; validation, C.Z., R.S., S.N.G. and K.S.; formal analysis, C.Z., S.N.G. and R.S.; investigation, S.N.G. and C.Z.; resources, C.Z., R.S. and S.N.G.; data curation, S.N.G. and C.Z.; writing—original draft preparation, C.Z.; writing—review and editing, R.S., S.N.G. and R.G.; visualization, C.Z.; supervision, K.S. and R.G.; project administration, C.Z. and R.G.; funding acquisition, R.G. All authors have read and agreed to the published version of the manuscript.

Funding: We are grateful to the sponsorship received from the following grants 69763, 77739, and 45779 to the department of Mechanical and Aerospace Engineering, UCLA.

Data Availability Statement: All sources of data have been cited in the article either directly or via a reference paper.

Conflicts of Interest: The authors declare no conflict of interest.

Appendix A

Table A1. Load flow of the IEEE 33 bus distribution network without MDHD EVs.

Bus Number	Voltage Magnitude (p.u.)	Active Power (kW)	Reactive Power (kVar)
1	1.000000	−3917.677	−2435.141
2	0.997032	100.000	60.000
3	0.982938	90.000	40.000
4	0.975456	120.000	80.000
5	0.968059	60.000	30.000
6	0.949658	60.000	20.000
7	0.946173	200.000	100.000
8	0.941328	200.000	100.000
9	0.935059	60.000	20.000
10	0.929244	60.000	20.000

Table A1. Cont.

Bus Number	Voltage Magnitude (p.u.)	Active Power (kW)	Reactive Power (kVar)
11	0.928384	45.000	30.000
12	0.926885	60.000	35.000
13	0.920772	60.000	35.000
14	0.918505	120.000	80.000
15	0.917093	60.000	10.000
16	0.915725	60.000	20.000
17	0.913698	60.000	20.000
18	0.913090	90.000	40.000
19	0.996504	90.000	40.000
20	0.992926	90.000	40.000
21	0.992222	90.000	040.000
22	0.991584	90.000	040.000
23	0.979352	90.000	050.000
24	0.972681	420.000	200.000
25	0.969356	100.000	200.000
26	0.947729	90.000	25.000
27	0.945165	120.000	25.000
28	0.933726	60.000	20.000
29	0.925507	60.000	70.000
30	0.921950	200.000	600.000
31	0.917789	200.000	70.000
32	0.916873	60.000	100.000
33	0.916590	60.000	40.000

References

- Razmjoo, A.; Ghazanfari, A.; Jahangiri, M.; Franklin, E.; Denai, M.; Marzband, M.; Garcia, D.A.; Maheri, A. A Comprehensive Study on the Expansion of Electric Vehicles in Europe. *Appl. Sci.* **2022**, *12*, 11656. [CrossRef]
- Langbroek, J.H.; Franklin, J.P.; Susilo, Y.O. The effect of policy incentives on electric vehicle adoption. *Energy Policy* **2016**, *94*, 94–103. [CrossRef]
- Kwong, J.; Salah, S.; Deboever, J.; Zhao, A.; Dunckley, J. 36th International Electric Vehicle Symposium and Exhibition: Medium and Heavy Duty Fleet Electrification Planning and Assessment, Sacramento, CA, USA, June 2023. Available online: [https://evs36.com/wp-content/uploads/finalpapers/FinalPaper_Kwong_Jennifer%20\(2\).pdf](https://evs36.com/wp-content/uploads/finalpapers/FinalPaper_Kwong_Jennifer%20(2).pdf) (accessed on 20 September 2023).
- Taylor, T. The Advance of the Advanced Clean Truck (ACT) Rule. Available online: <https://www.atlasevhub.com/weekly-digest/the-advance-of-the-act/#:~:text=The%20ACT%20requires%20manufacturers%20who,of%20the%20Clean%20Air%20Act> (accessed on 30 September 2023).
- Painuli, S.; Rawat, M.S.; Rao, G.K.; Rayudu, D.R. Effects on Distribution System Voltage Stability including Electric Vehicles and Its Enhancement by Placing DG at Optimal Location. 2018. Available online: <https://www.researchgate.net/publication/324648024> (accessed on 15 August 2023).
- El Helou, R.; Sivaranjani, S.; Kalathil, D.; Schaper, A.; Xie, L. The impact of heavy-duty vehicle electrification on large power grids: A synthetic Texas case study. *Adv. Appl. Energy* **2022**, *6*, 100093. [CrossRef]
- Hong, W.; Jenn, A.; Wang, B. Electrified autonomous freight benefit analysis on fleet, infrastructure and grid leveraging Grid-Electrified Mobility (GEM) model. *Appl. Energy* **2023**, *335*, 120760. [CrossRef]
- Vandael, S.; Claessens, B.; Ernst, D.; Holvoet, T.; Deconinck, G. Reinforcement Learning of Heuristic EV Fleet Charging in a Day-Ahead Electricity Market. *IEEE Trans. Smart Grid* **2015**, *6*, 1795–1805. [CrossRef]
- Danese, A.; Torsæter, B.N.; Sumper, A.; Garau, M. Planning of High-Power Charging Stations for Electric Vehicles: A Review. *Appl. Sci.* **2022**, *12*, 3214. [CrossRef]

10. Mahmud, N.; Zahedi, A. Review of control strategies for voltage regulation of the smart distribution network with high penetration of renewable distributed generation. *Renew. Sustain. Energy Rev.* **2016**, *64*, 582–595. [[CrossRef](#)]
11. Roy, N.; Pota, H.; Hossain, M. Reactive power management of distribution networks with wind generation for improving voltage stability. *Renew. Energy* **2013**, *58*, 85–94. [[CrossRef](#)]
12. Schiffer, J.; Seel, T.; Raisch, J.; Sezi, T. Voltage Stability and Reactive Power Sharing in Inverter-Based Microgrids With Consensus-Based Distributed Voltage Control. *IEEE Trans. Control Syst. Technol.* **2015**, *24*, 96–109. [[CrossRef](#)]
13. Nanibabu, S.; Shakila, B.; Prakash, M. Reactive Power Compensation using Shunt Compensation Technique in the Smart Distribution Grid. In Proceedings of the 2021 6th International Conference on Computing, Communication and Security (ICCCS), Las Vegas, NV, USA, 4–6 October 2021; pp. 1–6. [[CrossRef](#)]
14. Adewuyi, O.B.; Shigenobu, R.; Ooya, K.; Senjyu, T.; Howlader, A.M. Static voltage stability improvement with battery energy storage considering optimal control of active and reactive power injection. *Electr. Power Syst. Res.* **2019**, *172*, 303–312. [[CrossRef](#)]
15. Fusco, G.; Russo, M.; De Santis, M. Decentralized Voltage Control in Active Distribution Systems: Features and Open Issues. *Energies* **2021**, *14*, 2563. [[CrossRef](#)]
16. Mishra, M.K.; Lal, V.N. An improved methodology for reactive power management in grid integrated solar PV system with maximum power point condition. *Sol. Energy* **2020**, *199*, 230–245. [[CrossRef](#)]
17. De Santis, M.; Di Fazio, A.R.; Russo, M.; Harighi, T.; Borghetti, A. Voltage Optimization in Distribution Networks using EV Parking Lots and PV systems as flexibility options. In Proceedings of the 2023 IEEE International Conference on Environment and Electrical Engineering and 2023 IEEE Industrial and Commercial Power Systems Europe (EEEIC/I&CPS Europe), Madrid, Spain, 6–9 June 2023; pp. 1–6. [[CrossRef](#)]
18. Kisacikoglu, M.C.; Ozpineci, B.; Tolbert, L.M. EV/PHEV Bidirectional Charger Assessment for V2G Reactive Power Operation. *IEEE Trans. Power Electron.* **2013**, *28*, 5717–5727. [[CrossRef](#)]
19. Vittorias, I.; Metzger, M.; Kunz, D.; Gerlich, M.; Bachmaier, G. A bidirectional battery charger for electric vehicles with V2G and V2H capability and active and reactive power control. In Proceedings of the 2014 IEEE Transportation Electrification Conference and Expo (ITEC), Dearborn, MI, USA, 15–18 June 2014; pp. 1–6. [[CrossRef](#)]
20. Lenka, R.K.; Panda, A.K.; Dash, A.R.; Venkataramana, N.N.; Tiwary, N. Reactive Power Compensation using Vehicle-to-Grid enabled Bidirectional Off-Board EV Battery Charger. In Proceedings of the 2021 1st International Conference on Power Electronics and Energy (ICPEE), Bhubaneswar, India, 2–3 January 2021; pp. 1–6. [[CrossRef](#)]
21. Li, Y.; Li, L.; Peng, C.; Zou, J. An MPC based optimized control approach for EV-based voltage regulation in distribution grid. *Electr. Power Syst. Res.* **2019**, *172*, 152–160. [[CrossRef](#)]
22. Hu, J.; Yin, W.; Ye, C.; Bao, W.; Wu, J.; Ding, Y. Assessment for Voltage Violations considering Reactive Power Compensation Provided by Smart Inverters in Distribution Network. *Front. Energy Res.* **2021**, *9*, 713510. [[CrossRef](#)]
23. Nazaripouya, H.; Pota, H.R.; Chu, C.-C.; Gadh, R. Real-Time Model-Free Coordination of Active and Reactive Powers of Distributed Energy Resources to Improve Voltage Regulation in Distribution Systems. *IEEE Trans. Sustain. Energy* **2019**, *11*, 1483–1494. [[CrossRef](#)]
24. Nassef, A.M.; Abdelkareem, M.A.; Maghrabie, H.M.; Baroutaji, A. Review of Metaheuristic Optimization Algorithms for Power Systems Problems. *Sustainability* **2023**, *15*, 9434. [[CrossRef](#)]
25. Lu, P.; Ye, L.; Zhao, Y.; Dai, B.; Pei, M.; Tang, Y. Review of meta-heuristic algorithms for wind power prediction: Methodologies, applications and challenges. *Appl. Energy* **2021**, *301*, 117446. [[CrossRef](#)]
26. Antarasee, P.; Premrudeepreechacharn, S.; Siritaratiwat, A.; Khunkitti, S. Optimal Design of Electric Vehicle Fast-Charging Station's Structure Using Metaheuristic Algorithms. *Sustainability* **2022**, *15*, 771. [[CrossRef](#)]
27. Mazumder, M.; Debbarma, S. EV Charging Stations with a Provision of V2G and Voltage Support in a Distribution Network. *IEEE Syst. J.* **2020**, *15*, 662–671. [[CrossRef](#)]
28. Gandhi, O.; Zhang, W.; Rodriguez-Gallegos, C.D.; Srinivasan, D.; Reindl, T. Continuous optimization of reactive power from PV and EV in distribution system. In Proceedings of the 2013 IEEE Innovative Smart Grid Technologies-Asia (ISGT Asia), Bangalore, India, 10–13 November 2013; Volume 9, pp. 1–6, 281–287. [[CrossRef](#)]
29. Hemmatpour, M.H.; Koochi, M.H.R.; Dehghanian, P.; Dehghanian, P. Voltage and energy control in distribution systems in the presence of flexible loads considering coordinated charging of electric vehicles. *Energy* **2021**, *239*, 121880. [[CrossRef](#)]
30. Bakirtzis, A.G.; Biskas, P.N.; Zoumas, C.E.; Petridis, V. Optimal Power Flow by Enhanced Genetic Algorithm. *IEEE Trans. Power Syst.* **2002**, *17*, 229–236. [[CrossRef](#)]
31. del Valle, Y.; Venayagamoorthy, G.K.; Mohagheghi, S.; Hernandez, J.-C.; Harley, R.G. Particle Swarm Optimization: Basic Concepts, Variants and Applications in Power Systems. *IEEE Trans. Evol. Comput.* **2008**, *12*, 171–195. [[CrossRef](#)]
32. Taher, M.A.; Kamel, S.; Jurado, F.; Ebeed, M. An improved moth-flame optimization algorithm for solving optimal power flow problem. *Int. Trans. Electr. Energy Syst.* **2018**, *29*, e2743. [[CrossRef](#)]
33. Mirjalili, S.; Gandomi, A.H.; Mirjalili, S.Z.; Saremi, S.; Faris, H.; Mirjalili, S.M. Salp Swarm Algorithm: A bio-inspired optimizer for engineering design problems. *Adv. Eng. Softw.* **2017**, *114*, 163–191. [[CrossRef](#)]
34. Mirjalili, S.; Lewis, A. The Whale Optimization Algorithm. *Adv. Eng. Softw.* **2016**, *95*, 51–67. [[CrossRef](#)]
35. Mirjalili, S.; Mirjalili, S.M.; Lewis, A. Grey Wolf Optimizer. *Adv. Eng. Softw.* **2014**, *69*, 46–61. [[CrossRef](#)]
36. Al-Hanahi, B.; Ahmad, I.; Habibi, D.; Masoum, M.A.S. Charging Infrastructure for Commercial Electric Vehicles: Challenges and Future Works. *IEEE Access* **2021**, *9*, 121476–121492. [[CrossRef](#)]

37. Liimatainen, H.; van Vliet, O.; Aplyn, D. The potential of electric trucks—An international commodity-level analysis. *Appl. Energy* **2018**, *236*, 804–814. [[CrossRef](#)]
38. Zhang, C.; Sheinberg, R.; Gowda, S.N.; Sherman, M.; Ahmadian, A.; Gadh, R. A novel large-scale EV charging scheduling algorithm considering V2G and reactive power management based on ADMM. *Front. Energy Res.* **2023**, *11*, 1078027. [[CrossRef](#)]
39. Baran, M.E.; Wu, F.F. Network reconfiguration in distribution systems for loss reduction and load balancing. *IEEE Trans. Power Deliv.* **1989**, *4*, 1401–1407. [[CrossRef](#)]
40. Thurner, L.; Scheidler, A.; Schafer, F.; Menke, J.-H.; Dollichon, J.; Meier, F.; Meinecke, S.; Braun, M. Pandapower—An Open-Source Python Tool for Convenient Modeling, Analysis, and Optimization of Electric Power Systems. *IEEE Trans. Power Syst.* **2018**, *33*, 6510–6521. [[CrossRef](#)]
41. Smith, D.; Ozpineci, B.; Graves, R.L.; Jones, P.T.; Lustbader, J.; Kelly, K.; Walkowicz, K.; Birky, A.; Payne, G.; Sigler, C.; et al. *Medium-and Heavy-Duty Vehicle Electrification An Assessment of Technology and Knowledge Gaps*; Oak Ridge National Lab.(ORNL): Oak Ridge, TN, USA, 2019. [[CrossRef](#)]
42. National Renewable Energy Laboratory. End-Use Load Profiles for the U.S. Building Stock. Available online: <https://www.nrel.gov/buildings/end-use-load-profiles.html#dataset> (accessed on 15 February 2023).

Disclaimer/Publisher’s Note: The statements, opinions and data contained in all publications are solely those of the individual author(s) and contributor(s) and not of MDPI and/or the editor(s). MDPI and/or the editor(s) disclaim responsibility for any injury to people or property resulting from any ideas, methods, instructions or products referred to in the content.